RESEARCH NOTE

ACOUSTO-REFRIGERATOR WITH AN ADJUSTABLE MECHANICAL RESONATOR

A. Amjadi

Department of Physics, Sharif University of Technology
P.O. Box 11365-9161, Tehran, Iran
amjadi@sharif.edu

M. R. Abolhassani and S. Basir Jafari*

Department of Physics, Tarbiat Modares University
P.O. Box 14115-111, Tehran, Iran
taher40@yahoo.com - s_basirjafari@modares.ac.ir - basirjafari@irib.ir

*Corresponding Author

(Received: October 25, 2007 – Accepted in Revised Form: January 30, 2008)

Abstract Thermoacoustics describes energy conversion processes, activated by interaction temperature oscillation, accompanying the pressure oscillation in a sound wave, with solid boundaries. In ordinary experience this interaction of sound and heat cannot be observed, because of the very low temperature differences, but under suitable conditions, it can be emphasized and amplified to create remarkable thermodynamic effects such as, steep thermal gradients, powerful convective heat fluxes, and strong sound fields. We designed and constructed a simple thermoacoustic refrigerator with an adjustable mechanical resonator, coupled with the acoustic resonator. Our experimental data showed about % 10 increase in the efficiency of the refrigeration in comparison with a simple thermoacoustic refrigerator with no mechanical resonator.

Keywords Thermoacoustic Refrigerator, Stack, Resonator Tube, Drinking Straw, Coupled-mechanical Resonator, Nonlinear Spring

چکیده ترموآکوستیک، فرایند تبدیل انرژی حاصل از اندرکنش نوسان دمای جفت شده با نوسان فشار در یک موج صوتی که با مرزهای جامد در تماس است را توصیف می‌کند. در تجربه های عادی چنین اندرکنشی را نمی توان مشاهده کرد چون اختلاف دمای بسیار کمی ایجاد می‌شود ولی تحت شرایط مناسب با بهینه کردن سیستم آزمایشی می توان آن را تقویت کرد تا جاییکه اثرات ترمودینامیکی قابل توجهی همچون گرادیان های گرمایی تند، شارش های گرمایی قدرتمند و میدان های صوتی قوی را در اثر چنین اندرکنشی می توان نتیجه گرفت. ما یخچال ترموآکوستیکی ساده ای را طراحی کرده و ساختیم که یک رزوناتور مکانیکی قابل تنظیم جفت شده با رزوناتور آکوستیکی دارد. داده های آزمایشی ما افزایش راندمانی حدوداً ٪ ۱۰ در سرمایشَ سیستم، در مقایسه با یک یخچال ترموآکوستیکی ساده بدون رزوناتور مکانیکی نشان داد.

1. INTRODUCTION

It is absolutely imperative for our future to establish a basic technology for a cooling system attaining reduced size, light weight, high quality, most reliable, no use of poisonous gas and long life [1]. Thermoacoustics is the field concerned with transformations between thermal and acoustic energy. It has a long history that dates back to more than two centuries. For the most part heat driven oscillations were subject of these investigations. The reverse process, generating temperature differences using acoustic oscillations, is a relatively new phenomenon [2]. As shown in Figure 1, a refrigerator or heat pump absorbs heat Q_C at a low temperature T_C and requires the input

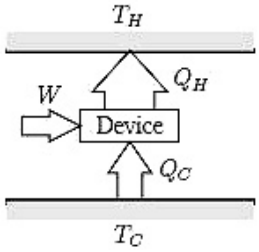

Figure 1. Refrigerator or heat pump.

of mechanical work W to exhaust more heat Q_H to a higher temperature T_H. The only difference between the purpose of a heat pump and a refrigerator is whether, the device is to extract heat at the lower temperature (refrigeration) or to reject heat at the higher temperature (heating).

Thermoacoustic refrigerators are devices that use acoustic power to transfer heat from low temperature to a high temperature source. Standing-wave thermoacoustic refrigerator is a much perused research area today and holds many potential applications in the power appliance, and space industries [3]. Typically, standing-wave thermoacoustic devices consist mainly of an acoustic resonator filled with a gas. In the resonator, a stack consisting of a number of parallel plates, and two heat exchangers, are appropriately installed. The main problem is the interaction between the porous medium (stack) and the sound field in the tube. The stack is the heart of the device where the thermoacoustic cycle is generated. In response to the acoustic wave, the gas in the tube oscillates, compressed and expanded. As a consequence, temperature gradient in the wave direction is produced. Since the gas contracts at high pressure and expands at low pressure, a net work of sound wave is prepared [4].

We have designed and constructed an acousto-refrigerator with an adjustable coupled mechanical resonator. This mechanical resonator with the acoustical resonator of the system are coupled in such a way that, a person can adjust the mechanical resonance frequency, to get a better efficiency from the refrigerator.

Nowadays, Thermoacoustic devices are well advanced and seem to have the immediate potential, to be used as an alternative to the conventional energy-conversion systems that are widely used as, internal combustion engine, steam turbine, vapor-compression refrigerator, gas turbine, and etc.

The power converter had been modeled and analyzed with Los Alamos National Lab. Scientists are studying, the miniaturization of thermoacoustic refrigerator [5,6]. There are many reference literatures available, such as [7,8].

Miniaturized thermoacoustic devices can be interfaced individually with the chips, on a microcircuit and can be stacked in an array to service the whole unit, whether it is a desktop or a portable system [9].

2. THEORY

This section is devoted to the analytical model describing the thermoacoustic devices. A detailed description of these systems and the way they work can be found in the literature [10]. Rienstra and Molenaar modeled the thermoacoustic refrigerator as depicted in Figure 2. It consists of a closed tube as a resonator and two heat exchangers. The other end of the resonator is driven by a loudspeaker. The porous medium is modeled as a stack of parallel plates; each has a thickness of 2l and length L. The space between the plates is equal to 2R.

In Figure 3 a portion of the tube wall (or a stack plate) is shown in Figure 2. The x-axis is along the direction of acoustic vibration and the y-axis perpendicular to the tube wall. The focus is, on what happens inside the stack.

The resulting refrigeration can be determined by examining a typical small element of gas, held between the plates of the stack. As the gas oscillates back and forth because of the existing sound wave, it changes in temperature. Much of the temperature changes, are created by gas expansion and compression, initiated by sound pressure (as always, is in a sound wave), and the rest is the consequence of heat transfer between the gas and the stack.

In the example shown, the length of the resonator is one-fourth the wavelength of the sound produced by the speaker, so all the elements of the gas are compressed and heated as they move to the left while expanded and cooled as they move to the right. Thus each element of the gas goes

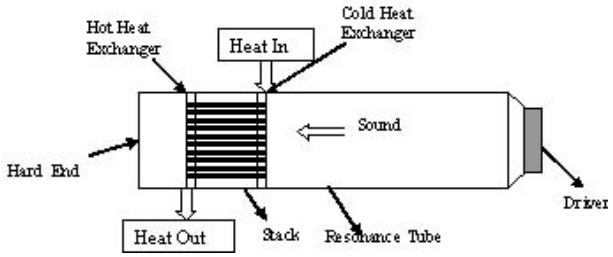

Figure 2. A simple illustration of a thermoacoustic refrigerator.

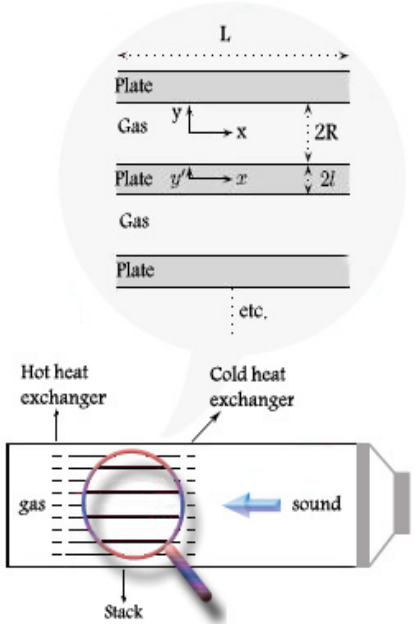

Figure 3. A thermoacoustic device modeled as an acoustically resonant tube, containing a gas, a stack of parallel plates and heat exchangers at both sides of the stack; without mechanical resonator.

through a thermodynamic cycle in which the element is compressed and heated, consequently rejects heat at the left end of the refrigerator. On the other hand at the right end of the system the gas is depressurized, cooled, and absorbs heat.

Consequently each element of the gas transfers a little heat from right to left or from cold to hot end of the tube during each cycle of the sound wave. The combination of all the gas element cycles, transports heat from the cold heat exchanger to the hot heat exchanger, like a bucket brigade transports water.

Rienstra, et al [10] used the dimensional analysis. This is a powerful tool in understanding physical effects which are governed by several dimensionless parameters and appear in the equations, such as the Mach number (A), the Prandtl number (Pr), the Laucret number (N_L) and several geometrical quantities.

The Laucret number is defined as the ratio of half porous size and the thermal penetration depth. If $N_L \geq 1$ the porous medium is called a stack. By carefully analyzing asymptotic situations in which these parameters differ in orders of magnitude, we can study the behavior of the system as a function of parameters associated with geometry, heat transport and viscous effects.

The first step would be to use "~" to indicate dimensional variables, and next we rescale the variables in equations in such way, that the equations become dimensionless. The general equations describing the thermodynamic behavior are [11]

$$\tilde{\rho}\left[\frac{\partial \tilde{V}}{\partial \tilde{t}}+\left(\tilde{V}\cdot\tilde{\nabla}\right)\tilde{V}\right]=-\tilde{\nabla}\tilde{p}+\mu\tilde{\nabla}^2\tilde{V}+\left(\xi+\frac{\mu}{3}\right)\tilde{\nabla}\left(\tilde{\nabla}\cdot\tilde{V}\right) \quad (1)$$

$$\frac{\partial \tilde{\rho}}{\partial \tilde{t}}+\tilde{\nabla}\cdot\left(\tilde{\rho}\tilde{V}\right)=0 \quad (2)$$

$$\tilde{\rho}c_p\left(\frac{\partial \tilde{T}}{\partial \tilde{t}}+\tilde{V}\cdot\tilde{\nabla}\tilde{T}\right)-\tilde{\beta}\tilde{T}\left(\frac{\partial \tilde{p}}{\partial \tilde{t}}+\tilde{V}\cdot\tilde{\nabla}\tilde{p}\right)=K\tilde{\nabla}\cdot\left(\tilde{\nabla}\tilde{T}\right)+\tilde{\Sigma}:\tilde{\nabla}\tilde{V} \quad (3)$$

$$d\tilde{\rho}=\frac{\gamma}{c^2}d\tilde{p}-\tilde{\rho}\tilde{\beta}d\tilde{T} \quad (4)$$

$$\tilde{\rho}_s c_s\frac{\partial \tilde{T}_s}{\partial \tilde{t}}=K_s\tilde{\nabla}^2\tilde{T} \quad (5)$$

The first, second, third and the last equations are "Navier-Stokes equation", "Continuity equation", "Energy equation" and "Diffusion equation", respectively. Here $\tilde{\rho}$ is the density, $\tilde{V}$ is the velocity, $\tilde{p}$ is the pressure, $\tilde{T}$ is the temperature, μ

and ζ are the dynamic (shear) and second (bulk) viscosity, respectively; K is the gas thermal conductivity, c_p is the specific heat per unit mass, $\tilde{\beta}$ is the thermal expansion coefficient. K_s, c_s and ρ_s are the thermal conductivity, the specific heat per unit mass and the density of the stack's material, respectively and $\tilde{\Sigma}_{ij}$ is the viscous stress tensor, with components

$$\tilde{\Sigma}_{ij} = \mu\left(\frac{\partial \tilde{v}_i}{\partial \tilde{x}_j} + \frac{\partial \tilde{v}_j}{\partial \tilde{x}_i} - \frac{2}{3}\delta_{ij}\frac{\partial \tilde{v}_k}{\partial \tilde{x}_k}\right) + \xi\delta_{ij}\frac{\partial \tilde{v}_k}{\partial \tilde{x}_k}. \quad (6)$$

These equations will be linearized and simplified using the following assumptions:

- The theory is linear; second-order effects, such as acoustic streaming and turbulence, are neglected.
- The plates are fixed and rigid.
- The temperature variations along the stack are much smaller than the absolute temperature.
- The temperature dependence of viscosity is neglected.
- Oscillating variables have harmonic time dependence at a single angular frequency $\tilde{\omega}$.

At the boundaries Rienstra, et al [10] imposed the no-slip condition

$$\tilde{V}\big|_{\tilde{y}=\pm R} = 0, \quad (7)$$

The temperatures of the plates and the gas are coupled at the solid-gas interface where continuity of temperature and heat fluxes is imposed:

$$\tilde{T}\big|_{\tilde{y}=\pm R} = \tilde{T}_s\big|_{\tilde{y}'=\mp l} =: \tilde{T}_b(x), \quad (8)$$

$$K\left(\frac{\partial \tilde{T}}{\partial \tilde{y}}\right)_{\tilde{y}=\pm R} = K_s\left(\frac{\partial \tilde{T}_s}{\partial \tilde{y}'}\right)_{\tilde{y}'=\mp l}. \quad (9)$$

They didn't impose any conditions at the stack ends, as were mainly interested in what happens inside the stack, ignoring any entrance effects.

They assumed a 2D-model and rescaled as follows

$$\begin{aligned}
&\tilde{x} = Lx, \tilde{y} = Ry, \tilde{y}' = ly', \tilde{u} = Cu, \tilde{\rho}_s = D_s\rho_s,\\
&\tilde{v} = \varepsilon Cv, \tilde{p} = DC^2 p, \tilde{\rho} = D\rho, \tilde{c} = Cc,\\
&\tilde{T}_s = \frac{C^2}{c_p}T_s, \tilde{\beta} = \frac{c_p\beta}{C^2}, \tilde{T} = \frac{C^2}{c_p}T, \tilde{t} = \frac{Lt}{C},
\end{aligned} \quad (10)$$

Where C is a typical speed of sound, D and D_s are typical densities for the fluid and solid, respectively, and ε is the ratio of the stack porous defined as $\varepsilon = (R/L) << 1$. Clearly, ε is a dimensionless parameter. In addition to ε, they used the following dimensionless parameters:

$$\begin{aligned}
&\varepsilon_1 = \frac{l}{L}, \theta = \frac{RK_s}{lK}, \omega = \frac{\tilde{\omega}L}{C}, \gamma = \frac{c_p}{c_v}, A = \frac{U}{C},\\
&W_o = \frac{\sqrt{2}R}{\delta_v}, N_L = \frac{R}{\delta_k}, N_s = \frac{l}{\delta_s}, \Pr = \frac{2N_L^2}{W_o},
\end{aligned} \quad (11)$$

Where c_v is the isochoric specific heat, $\tilde{\omega}$ is the frequency, $\lambda = 2\pi\tilde{c}/\tilde{\omega}$ is the wavelength, U is a typical fluid speed, A is a Mach number, Pr is the Prandtl number, W_0 is the Womersley number and N_L and N_s are the Laucret numbers associated with the fluid and the solid, respectively. Here parameters δ_v, δ_k and δ_s are the viscous penetration depth, and the thermal penetration depths for the fluid and solid, respectively.

$$\delta_v = \sqrt{\frac{2\nu}{\tilde{\omega}}}, \ \delta_k = \sqrt{\frac{2\kappa}{\tilde{\omega}}}, \ \delta_s = \sqrt{\frac{2\kappa_s}{\tilde{\omega}}}. \quad (12)$$

Here $\nu = \mu/D$ is the kinematic viscosity and $\kappa = K/(Dc_p)$ is the thermal diffusivity of the fluid. The first eight of the dimensionless parameters in Equation 11 together with ε form nine independent dimensionless parameters.

In dimensionless form the x-component of the momentum equation and the y-component are obtained as follows [10]

$$\begin{aligned}
&\rho\left(\frac{\partial u}{\partial t} + u\frac{\partial u}{\partial x} + v\frac{\partial u}{\partial y}\right) = -\frac{\partial p}{\partial x} + \frac{\omega}{W_o^2}\left(\varepsilon^2\frac{\partial^2 u}{\partial x^2} + \frac{\partial^2 u}{\partial y^2}\right)\\
&+ \frac{\varepsilon\omega}{W_o^2}\left(\frac{\xi}{\mu} + \frac{1}{3}\right)\left(\frac{\partial^2 u}{\partial x^2} + \frac{\partial^2 v}{\partial x\partial y}\right),
\end{aligned} \quad (13)$$

$$\varepsilon^2\rho\left(\frac{\partial v}{\partial t}+u\frac{\partial v}{\partial x}+v\frac{\partial v}{\partial y}\right)=-\frac{\partial p}{\partial y}+\frac{\varepsilon^2\omega}{{W_o}^2}$$
$$\left(\varepsilon^2\frac{\partial^2 v}{\partial x^2}+\frac{\partial^2 v}{\partial y^2}\right)+\frac{\varepsilon^2\omega}{{W_o}^2}\left(\frac{\xi}{\mu}+\frac{1}{3}\right)\left(\frac{\partial^2 u}{\partial x\partial y}+\frac{\partial^2 v}{\partial y^2}\right). \quad (14)$$

The continuity equation and the energy equation will be

$$\frac{\partial\rho}{\partial t}+\frac{\partial(\rho u)}{\partial x}+\frac{\partial(\rho v)}{\partial y}=0, \quad (15)$$

and

$$\rho\left(\frac{\partial T}{\partial t}+u\frac{\partial T}{\partial x}+v\frac{\partial T}{\partial y}\right)-\beta T\left(\frac{\partial p}{\partial t}+u\frac{\partial p}{\partial x}+v\frac{\partial p}{\partial y}\right)$$
$$=\frac{\omega}{2{N_L}^2}\left(\varepsilon^2\frac{\partial^2 T}{\partial x^2}+\frac{\partial^2 T}{\partial y^2}\right)+\frac{\omega}{{W_o}^2}\left[\left(\frac{\partial u}{\partial y}\right)^2+O(\varepsilon)\right]. \quad (16)$$

The state equation and the diffusion equation have the form of

$$\rho_1=-\rho_0\beta T_1+\left(\frac{\gamma}{c^2}\right)p_1, \quad (17)$$

$$\rho_s\frac{\partial T_s}{\partial t}=\frac{\omega}{2{N_s}^2}\left({\varepsilon_1}^2\frac{\partial^2 T_s}{\partial x^2}+\frac{\partial^2 T_s}{\partial y'^2}\right). \quad (18)$$

Subject to

$$V\big|_{y=\pm1}=0, \quad (19)$$

$$T\big|_{y=\pm1}=T_s\big|_{y'=\mp1}=:T_b(x), \quad (20)$$

$$\left(\frac{\partial T}{\partial y}\right)_{y=\pm1}=\theta\left(\frac{\partial T_s}{\partial y'}\right)_{y'=\mp1}. \quad (21)$$

The prandtl number depends only on material parameters and is usually close to 1. As a result N_L and W_0 should be of the same order of magnitude. Normally in standing wave machines R ~ δ_k (stack), so N_L ~ 1 and W_0 ~1. Furthermore we assume that the amplitude of the acoustic oscillations can be taken arbitrarily small, with the restriction that $\varepsilon^2 << A$. We have

$$\theta = O(1),\ N_L \sim 1,\ W_0 \sim 1,\ \varepsilon_l^2 << \varepsilon^2 << A << \omega^2 << 1.$$

The presence of ω as a small parameter suggests the following alternative expansions for the fluid variables q

$$q(x,y,t)=q_0(x,y)+A\mathrm{Re}\left(q_1(x,y,t)\right)+...,$$
$$q_1(x,y,t)=\left(q_{10}(x,y)+\omega q_{11}(x,y)+...\right)e^{i\omega t}. \quad (22)$$

From Equations 13 and 14 the zeroth order equation yields $\partial p_0/\partial x=0$ and $\partial p_0/\partial y=0$. Combining terms of order A we can find that $\partial p_{10}/\partial x=0$. Next, combining the terms of order $A\omega^2$ and applying the boundary conditions $u_l(x, \pm 1) = 0$, we can obtain

$$u_{11}(x,y)=\frac{i}{\rho_0}\frac{dp_{12}}{dx}\left[1-\frac{\mathrm{Cosh}\left(\alpha_\nu y\right)}{\mathrm{Cosh}\left(\alpha_\nu\right)}\right],$$
$$\alpha_\nu=(1+i)\sqrt{\rho_0}\frac{R}{\delta_\nu}=(1+i)\sqrt{\frac{\rho_0}{2}}W_o. \quad (23)$$

The zeroth order Equation 16 yields $\partial^2 T_0/\partial y^2=0$ and by imposing the symmetry we can find that T_0 is in fact constant in y. Combining terms of order A, we can find

$$\rho_0 u_{10}\frac{dT_0}{dx}=0\Rightarrow\begin{cases}u_{10}=0\\ dT_0/dx=0\end{cases} \quad (24)$$

Finally, combining terms of order Aω and applying the boundary conditions in Equations 19, 20 and 21 we can obtain

$$T_{10}(x,y)=$$
$$\frac{\beta T_0 p_{10}}{\rho_0}-\frac{1}{\rho_0}\frac{dT_0}{dx}\frac{dp_{12}}{dx}\left[1-\frac{\mathrm{Pr}}{\mathrm{Pr}-1}\frac{\mathrm{Cosh}\left(\alpha_\nu y\right)}{\mathrm{Cosh}\left(\alpha_\nu\right)}\right]-$$

$$\left[\frac{\beta T_0 p_{10}}{\rho_0}+\frac{1}{\rho_0}\frac{1+\varepsilon_s}{Pr-1}\frac{f_\nu}{f_k}\right]\frac{Cosh\left(\alpha_k y\right)}{\left(1+\varepsilon_s\right)Cosh\left(\alpha_k\right)}, \quad (25)$$

Where

$$\alpha_k=(1+i)\sqrt{\rho_0}\,\frac{R}{\delta_k}=(1+i)\sqrt{\rho_0}\,N_L \quad (26)$$

$$f_k=\frac{tgh\left(\alpha_k\right)}{\alpha_k},f_\upsilon=\frac{tgh\left(\alpha_\upsilon\right)}{\alpha_\upsilon},$$
$$\varepsilon_s=\frac{\sqrt{K\tilde{\rho}_0 c_p}\,tgh\left(\alpha_k\right)}{\sqrt{K_s\tilde{\rho}_{s_0}c_s}\,tgh\left(\alpha_s\right)}. \quad (27)$$

In order to derive Rott's wave equation, we start with the continuity Equation 15. In spite of generally $v\neq 0$, combining terms of order A we find that $v_{10}=0$. In view of symmetry v(x,0) = 0 and restricted to terms of order up to Aω, from Equation 17 and substituting $c^2\beta^2T_0 = \gamma - 1$ finally Rott's wave equation (dimensionless) is written as [10]

$$\frac{1}{c^2}\left[1+\frac{\gamma-1}{1+\varepsilon_s}f_k\right]p_{10}+\frac{f_k-f_\nu}{(Pr-1)\left(1+\varepsilon_s\right)}\beta$$
$$\frac{dT_0}{dx}\frac{dp_{12}}{dx}+\rho_0\frac{d}{dx}\left(\frac{1-f_\nu}{\rho_0}\frac{dp_{12}}{dx}\right)=0. \quad (28)$$

The time-averaged acoustic power $d\dot{\tilde{W}}$ used (or produced in the case of a prime mover) in a segment of length dx can be calculated from

$$\frac{d\dot{\tilde{W}}}{dx}=\tilde{A}_g\frac{d}{d\tilde{x}}\left[\overline{\left\langle\tilde{p}_1'\tilde{u}_1'\right\rangle}\right], \quad (29)$$

Where the overbar indicates time average (over one period), brackets $\langle\ \rangle$ indicate averaging in the $\tilde{y}$-direction and $\tilde{A}_g$ is the cross-sectional area of the gas within the stack. Next $\dot{\tilde{W}}$ and $\tilde{A}_g$ are rescaled as $\dot{\tilde{W}}=R^2DC^3\dot{W}$ and $\tilde{A}_g=R^2A_g$. As p is independent of y, the rescaled time-averaged acoustic power in a segment of length dx is written as [10]

$$\frac{d\dot{W}}{dx}=$$
$$A^2A_g\frac{d}{dx}\left[\overline{p_1'\left\langle u_1'\right\rangle}\right]=\frac{1}{2}A^2A_gRe\left(\frac{d}{dx}\left[p_1\left\langle u^*{}_1\right\rangle\right]\right), \quad (30)$$

Where the star denotes complex conjugation. Restricted to terms of order up to $A\omega^2$, since $u_{10} = 0$ and $\partial p_{10}/\partial x=0$ we can obtain:

$$\frac{d\dot{W}_{21}}{dx}=\frac{A_g}{2}\left[\frac{(\gamma-1)Im\left(f_k\right)}{\rho_0c^2\left(1+\varepsilon_s\right)}\left|p_{10}\right|^2-\frac{\beta}{Pr-1}\right.$$
$$\left.\frac{dT_0}{dx}Re\left(\frac{f_k{}^*-f_\nu{}^*}{\left(1+\varepsilon_s{}^*\right)\left(1-f_\nu{}^*\right)}p_{10}\left\langle u^*{}_{11}\right\rangle\right)\right]. \quad (31)$$

Where the subscript 21 is used to indicate second order in A and first order in ω. The first term is the thermal relaxation dissipation term. This term is present whenever a wave interacts with a solid surface, and has a dissipative effect in thermoacoustics. The second term contains the temperature gradient dT_0/dx and is called the source term because it absorbs acoustic power in refrigerator. This term is the unique contribution to thermoacoustics.

Dissipation is usually undesirable, so the dissipation terms should be smaller than the source term. This gives the inequalities

$$\omega << N_L << 1. \quad (32)$$

If ω and N_L satisfy this equation, viscous and thermal relaxation dissipation can be neglected with respect to the source term. In other words reducing the porous size reduces the thermal relaxation dissipation and increases the viscous dissipation. However, the latter can be prevented by taking the stack short enough, as indicated in 32.

For improving the efficiency of this refrigerator we have designed and constructed an acousto-refrigerator with an adjustable coupled mechanical

resonator. This mechanical resonator is coupled with the acoustical resonator of the system in such a way that a person can adjust the mechanical resonance frequency, to get better efficiency from the refrigerator.

We can reduce a simple acoustic system to an analogous simple oscillator, i.e. a mechanical system having lumped mechanical elements of mass, resistance and stiffness.

The final equation of motion corresponds to the equation of motion for a forced oscillation of a mechanical system with damping:

$$\tilde{M}_a\ddot{\tilde{X}} + \tilde{R}_a\dot{\tilde{X}} + \tilde{k}_a\tilde{X} = \tilde{P}_0\tilde{S}\sin\tilde{\omega}\tilde{t}, \quad (33)$$

Where $\tilde{M}_a = \tilde{\rho}\tilde{L}/\tilde{S}$ is the acoustical mass, $\tilde{R}_a = \tilde{\rho}\tilde{c}^2\tilde{k}^2/(2\pi)$ is the acoustical resistance, $k_a = \tilde{\rho}\tilde{c}^2/\tilde{V}$ is the acoustical stiffness ($\tilde{C}_a = 1/\tilde{k}_a = \tilde{V}/\tilde{\rho}\tilde{c}^2$ is the acoustical compliance), $\tilde{k} = \tilde{\omega}/\tilde{c}$ is the wave number, $\tilde{S}$ is the cross-sectional area and $\tilde{V}$ is the volume of the tube. $\tilde{X}$ is displacement that equals to the particles displacement in the acoustical resonator and $\tilde{P}_0 \sin\tilde{\omega}\tilde{t}$ is the harmonic acoustic pressure. The study state acoustical oscillation is therefore given by [12]

$$\tilde{X}(\tilde{t}) = \frac{\tilde{P}_0}{\tilde{R}_a + i\left(\tilde{\omega}\tilde{M}_a - \frac{1}{\tilde{\omega}\tilde{C}_a}\right)}, \quad (34)$$

Where the denominator represents the acoustic impedance. Resonance or maximum volume velocity (air flow) in the neck occurs at a frequency which makes the total reactance zero, i.e.

$$\tilde{\omega}\tilde{M}_a - \frac{1}{\tilde{\omega}\tilde{C}_a} = 0,$$

or

$$\tilde{\omega} = \sqrt{\frac{1}{\tilde{M}_a\tilde{C}_a}}\ \text{rad}/\text{sec}. \quad (35)$$

We added an adjustable coupled mechanical resonator to this acoustical resonator that the mechanical resonator's equation is

$$\tilde{M}\ddot{\tilde{X}} + \tilde{k}_{spring}\tilde{X} = \tilde{P}_0\tilde{S}\sin\tilde{\omega}\tilde{t}, \quad (36)$$

Where $\tilde{M}$ the mass of a stainless steel disc is, $\tilde{k}_{spring}$ is the stiffness of the spring that consists of a linear $\tilde{k}_1$ and a nonlinear $\tilde{k}_2$ spring that hold the disc $\tilde{M}$ at the end of the refrigerator acoustical cavity. So we have a coupled oscillator.

As it is shown in Figure 4 applying force to the spring's system with an adjustable screw, changes the spring constant $\tilde{k}_2$ of the mechanical resonator. The study state mechanical oscillation is therefore given by [13]

$$\tilde{X} = \frac{\tilde{P}_0\tilde{S}}{\tilde{M}}\frac{\text{Cos}(\tilde{\omega}\tilde{t})}{\tilde{\omega}_0{}^2 - \tilde{\omega}^2}, \quad (37)$$

Where $\tilde{\omega}_0 = \sqrt{\tilde{k}_{spring}/\tilde{M}}$ is the resonance frequency of this mechanical resonator that $\tilde{k}_{spring} = \tilde{k}_1 + \tilde{k}_2$.

The acoustical resonance of the resonator $\tilde{f}_a$ is kept constant and the mechanical resonance of the driver $\tilde{f}_a$ is varied by changing the stiffness $\tilde{k}_2$. As the mechanical resonance frequency of the driver $\tilde{f}_d$ is shifted towards the acoustical resonance, the temperature gradient around the stack grows.

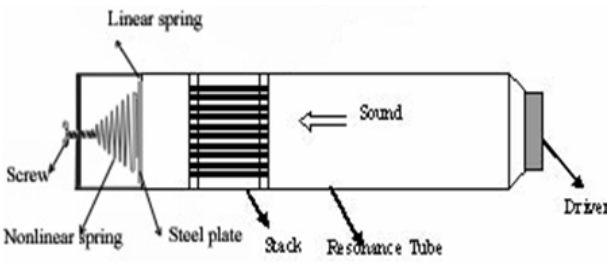

Figure 4. A simple illustration of a thermoacoustic refrigerator with an adjustable coupled mechanical resonator at the end of the resonator tube.

So the efficiency can always be made maximal by matching the mechanical and acoustical resonator frequencies. Therefore we were able to tune the system and get % (10 ± 3) better efficiency. This is an important improvement.

3. EXPERIMENTAL SET-UP

As discussed previously, the resonator consists of a tube which contains the stack and two heat exchangers. The design and material requirements for the stack, which forms the heart of the refrigerator, are important. Because of the difficulty of construction and the fragility of the parallel-plate stack, an approximate geometry is usually used [14], which consists of a long sheet winding around a rod to get a spiral stack.

The spacing between the layers is realized by fishing line spacers glued onto the surface of the sheet. The gaps between the layers are considered to approximate the parallel-plate channels. But we choose the simplest stack which consists of parallel drinking straws. Our thermoacoustic experimental set-up is shown in Figure 5.

The resonator was built from a straight glass tube of 100 cm length, internal diameter 2.7 cm and wall thickness of 1 mm. The working fluid was air at atmospheric pressure. One extremity of the tube was sealed up by a steel plate 3 cm thick; it constitutes the rigidity of the resonator.

We placed a screw connected to a nonlinear spring at this extremity of the tube. The other end of the spring is connected to a steel plate of 1 mm thick with electrical nonconductor perimeter of mass 4.45 gr that is shown in Figure 6.

The stack consists of parallel drinking straws, of inner diameter 2.7 mm. The stack has a diameter of 2.7 cm and a length of 3.8 cm, and can easily be installed inside the resonator tube.

The other end the resonator is driven by a loudspeaker. The resonator is connected to the loudspeaker box with a flange that is connected to a steel tube with 27.5 cm length. The system is not thermally insulated, and can simply be set on a table to demonstrate thermoacoustic refrigerator. So, the measurements are qualitative. A copper-constantan thermocouple is used to measure the temperature difference over the stack.

Figure 5. Experimental set-up of thermoacoustic refrigerator.

Figure 6. An adjustable coupled mechanical resonator that we added to the end of the resonator tube of thermoacoustic refrigerator. It consists of a screw connected to a nonlinear spring at the end of the tube. The other end of the spring is connected to a metal plate with electrical nonconductor perimeter.

As illustrated in Figure 7, the temperature difference is measured by fixing each copper-constantan junction of the thermocouple on opposite ends of the stack. Really a micro-voltmeter is used to measure the voltage difference, due to the temperature difference among the stack.

The position of the stack in the resonator tube relative to the existing wave is an important factor in the design of the existing wave-thermoacoustic

devices that, the position is chosen 4 cm away from the closed end of the tube.

4. EXPERIMENTAL RESULTS

In the present work, on the basis of the linear thermoacoustic theory, a simple calculus procedure has been outlined in order to investigate the origin of the prediction's deviation, of the linear theory from the measured performances of real devices. The spacing between the plates or the inner diameter of the drinking straws in the stack is crucial to function properly.

If the spacing or the diameter is too small, the good thermal contact between the gas and the stack keeps the gas at nearly the same temperature as the stack, whereas if the spacing or the diameter is too wide, much of the gas is in poor thermal contact with the stack and does not transfer heat effectively to and from it.

In the present work, an experiment on the thermoacoustic effect has been carried out, making use of structures and apparatus, as simple as possible in order to facilitate the interpretation of the experimental results.

First, the acoustic resonance frequency must be determined. It can be determined by measuring a resonance spectrum of the resonator, without any mechanical resonator, by making a low-power frequency sweep. We took the sound within the tube with a microphone and gave it to "Adobe Audition" a software for analysis.

The pressure amplitude of the signal is recorded over the sweep interval as function of the frequency. Whenever resonance takes place a peak shows up.

Therefore it was observed that a fundamental resonance frequency is about 300 Hz which is presented in Figure 8.

This figure is the frequency analysis of that signal is recorded over the sweep interval. The x-axis (left to right) represents frequency (measured in Hz), while the y-axis (bottom to top) corresponds to the amplitude of the corresponding frequency (measured in dB) on the x-axis.

After this we added an adjustable coupled mechanical resonator to this acoustical resonator as discussed previously.

By twisting the screw at the end of the tube, by changing the stiffness k_2, we tried to shift the mechanical resonance frequency towards the acoustical fundamental resonance frequency. Whenever matching takes place a peak shows up at the temperature gradient around the stack that is presented in Figure 9.

Then refrigerator is allowed to cool down and stabilize. We measured the temperature difference among the stack, indirectly with a micro-voltmeter (1 mV/10˚C). Typical measurement result is presented in Figure 9.

As illustrated in Figure 10, a peak takes place at the Fourier transform of the sound inside the system at 250 Hz but the pressure amplitude of the signal is lower than the amplitude at 300 Hz illustrated in Figure 11.

So the temperature gradient around the stack at 250 Hz and the other frequencies is lower than the temperature gradient at the fundamental resonance frequency (300 Hz) of the resonator. Typical measurement result of voltage gradient around the stack at several frequencies is presented in Figure 12.

5. DISCUSSION

One way in which sound waves are affected near solid boundaries is by viscosity and thermal-relaxation. This has a negative effect on the performance of thermoacoustic systems. The viscous losses are due to the viscosity that dissipates acoustic energy by viscous shear in the viscous boundary. The viscous dissipation is well known. To reduce the effect of viscosity, and hence to improve the performance of thermoacoustic systems, gas-mixtures with a low Prandtl number can be used. This has resulted in a 70 % improvement of the performance of a thermoacoustic refrigerator [15].

The thermal-relaxation loss is due to dissipation of the acoustic energy in the thermal boundary layer. The magnitude of this effect depends on the temperature difference between the core of the gas and the solid boundary. Although an analytical expression for the thermo-viscous dissipation was derived [11], a detailed analysis of the thermal-relaxation dissipation and possible solution to

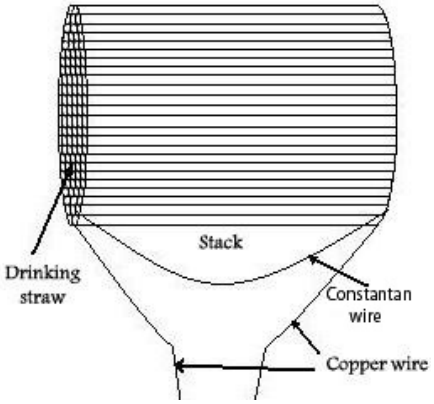

Figure 7. The stack is made of drinking straws glued together. A constantan-copper thermocouple is used to measure the temperature difference over the stack.

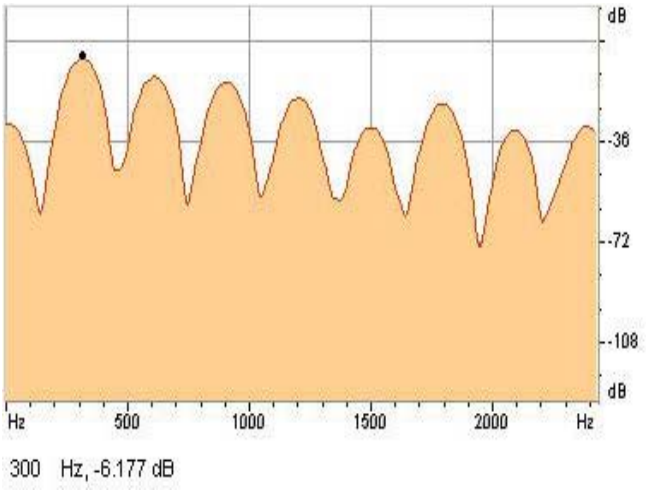

Figure 8. Resonance spectrum of the resonator without any mechanical resonator by making a low-power frequency sweep.

reduce its negative effect on thermoacoustic systems is still lacking.

Because the loss of acoustic energy has a negative effect on the efficiency of thermoacoustic systems, it is important to minimize this dissipation process. Reference [15] is devoted to the minimization of the thermal-relaxation dissipation in thermoacoustic systems. Contrary to the expression of the acoustic energy dissipated by thermal-relaxation, we note that the expression of the energy dissipated by viscous shear does not depend on the parameters of the wall material [11]. This means that walls of different materials but same smooth surfaces will cause the same viscous dissipation for the same flow conditions. The choice of a solid material with the smallest possible heat capacity per unit area, in combination with a gas with the largest possible heat capacity per unit area, minimizes the thermal-relaxation dissipation. Among different combinations of solid-gas used in the calculations, the combination cork-helium leads to the lowest thermal attenuation of the sound wave. However, because of the porosity of cork

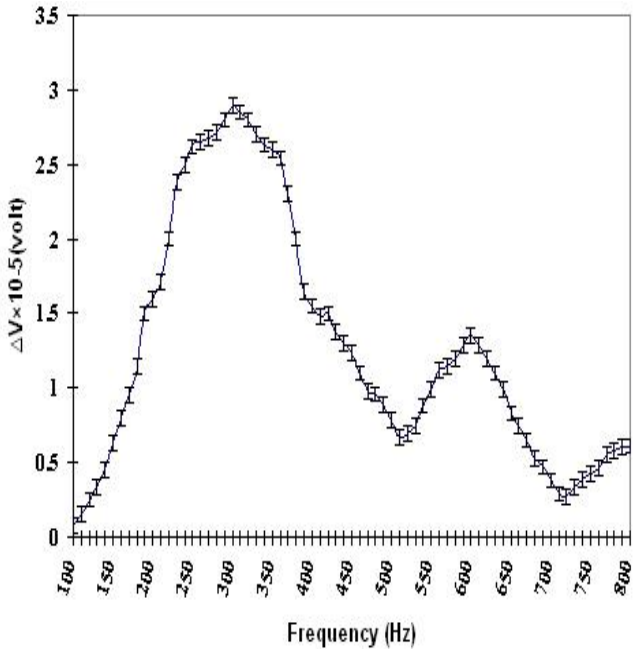

Figure 9. The voltage gradient is measured around the stack as a function of frequency at 15 dB, during the sweep of frequency from 100 Hz to 800 Hz in the resonator tube that we added an adjustable mechanical resonator to it. The error bar at this curve is 0.05×0^{-5} volt.

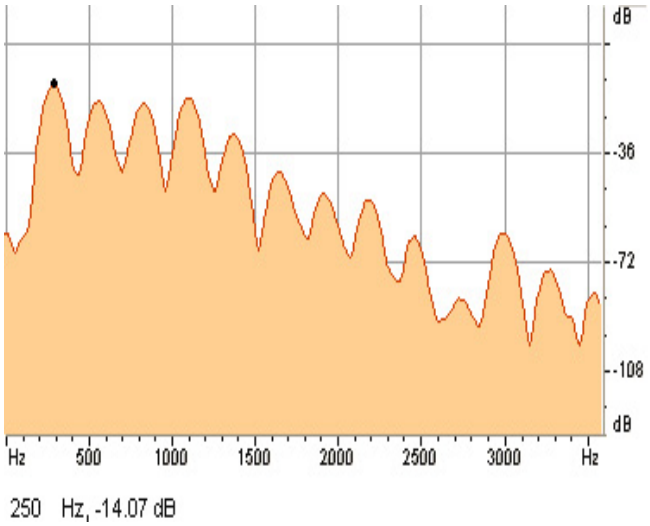

Figure 10. The Fourier transform of the sound inside the system at 250 Hz.

which may cause some problems, it is suggested that, the combination of polyester-helium to be used in practice, to minimize the thermal-relaxation losses.

It must however, be noticed that the reliability of data suffers (in addition of the experimental uncertainty which, anyway, does not justify the observed deviations) from intrinsic limitations

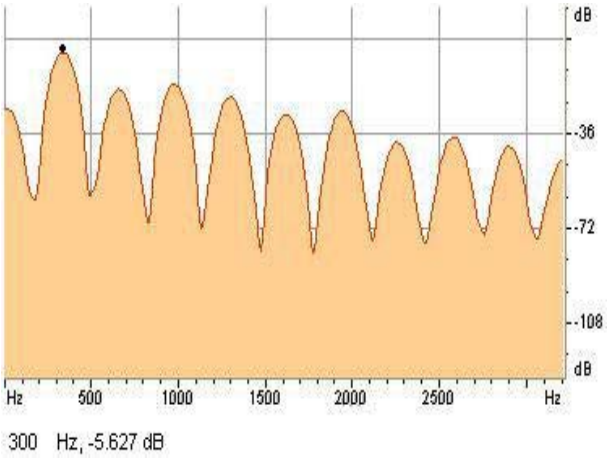

Figure 11. The Fourier transform of the sound inside the system at 300 Hz.

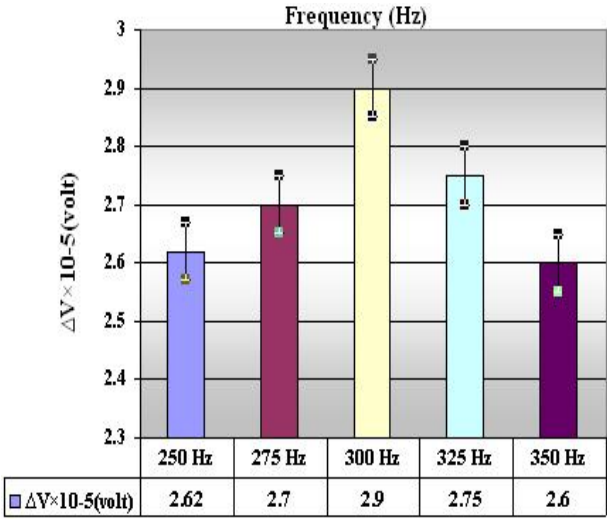

Figure 12. Comparison of the voltage gradient around the stack at several frequencies.

which may be due to the following causes:

- Nonlinear effects (presence of harmonics greater than the fundamental frequency);
- Turbulent flow, vortex generation, jetting (which can become relevant at the stack ends);
- Spurious heat leaks from the outside (the resonator tube was not insulated from the surrounding);
- Heat generated by viscous losses in the resonator walls and carried to the stack by acoustic streaming (this time-averaged convective heat flux constitutes an additional thermal load to the cold end of the stack);
- Heat fluxes in the transverse y direction (contrarily to what is assumed by the standard theory of thermoacoustics, the time-average temperature of the fluid could be different from that of the adjacent stack-walls);
- Heat transfer at the ends of the stack (the hypothesis of a perfectly isolated stack, i.e., one for which no heat is allowed to enter or leave either transversally or axially through the ends, could not hold).

6. CONCLUSIONS

We have designed and constructed an acousto-refrigerator with an adjustable coupled mechanical resonator. This mechanical resonator with the acoustical resonator of the system is coupled in such a way that, a person can adjust the mechanical resonance frequency to get better efficiency from the refrigerator.

The mechanical resonator consists of, a stainless steel disc with mass $\tilde{M}$ connected to a nonlinear spring. The spring consists of a linear and a nonlinear spring that holds the disc $\tilde{M}$ at the end of the refrigerator acoustical cavity. Appling force to the springs system with an adjustable screw, changes the spring constant of the mechanical resonator.

By changing the spring constant $\tilde{k}_{spring}$ and recording the temperature gradient and the fourier transform of the sound, inside the system at different frequencies, we were able to tune the system and get about % (10 ± 3) better efficiency.

So the acoustical resonance of the resonator $\tilde{f}_a$ is kept constant and the mechanical resonance of the driver $\tilde{f}_a$ is varied by changing the stiffness $\tilde{k}_2$. As the mechanical resonance frequency of the driver $\tilde{f}_d$ is shifted towards the acoustical resonance, the temperature gradient around the stack grows.

Therefore maximum efficiency can always be achieved by matching the mechanical and acoustical resonator frequencies. Hence, it was possible to tune the system and get % (10 ± 3) better efficiency. This is an important improvement.

7. NOMENCALTURE

7.1. Sub-and Superscripts

~	Dimensional Variable
C	Cold
H	Hot
s	Solid, Sink, Source
δ	Boundary Layer
ν	Viscous

7.2. General Constants and Variables

C	Typical Speed of Sound
$\tilde{c}$	Speed of Sound
$\tilde{C}_a$	Acoustical Compliance
c_p	Isobaric Specific Heat Per Unit Mass
c_v	Isochoric Specific Heat Per Unit Mass
c_s	Specific Heat Per Unit Mass of the Stack
D	Typical Density for the Fluid
D_s	Typical Density for the Solid
$\tilde{f}_a$	Acoustical Resonance of the Resonator
$\tilde{f}_d$	Mechanical Resonance of the Driver
$\tilde{k}_1$	Linear Spring Stiffness
$\tilde{k}_2$	Nonlinear Spring Stiffness
K	The Gas Thermal Conductivity
$\tilde{k}$	Wave Number
$\tilde{k}_a$	Acoustical Stiffness
K_s	Thermal Conductivity of the Stack
$\tilde{k}_{spring}$	Spring Stiffness
l	Plate Half-Thickness
L	Length of the Stack Plates
$\tilde{M}$	Mass of the Disk
$\tilde{M}_a$	Acoustical Mass
$\tilde{p}$	Pressure
Q_C	Heat Absorption at a Low Temperature
Q_H	Heat Absorption at a High Temperature
$\tilde{R}_a$	Acoustical Resistance
$\tilde{S}$	Cross-Sectional Area of the Tube
T_C	Low Temperature
T_H	High Temperature
$\tilde{t}$	Time
$\tilde{T}$	Temperature
U	Typical Fluid Speed
$\tilde{u}$	Velocity Component in Direction of Sound Propagation
$\tilde{V}$	Volume of the Resonator Tube
$\tilde{v}$	Velocity Component Perpendicular

	to the Direction of Sound Propagation
$\dot{\tilde{W}}$	Acoustic Power
$\tilde{x}$	Space Coordinates along Sound Propagation
$\tilde{X}$	Spring Displacement
$\dot{\tilde{X}}$	Spring Velocity
$\ddot{\tilde{X}}$	Spring Acceleration
$\tilde{y}$	Spaces Coordinate Perpendicular to Sound Propagation
R	Plate Half-Separation
$\tilde{\beta}$	Isobaric Volumetric Expansion Coefficient
δ_v	Viscous Penetration Depth
δ_k	Thermal Penetration Depth for the Fluid
δ_s	Thermal Penetration Depth for the Solid
κ	Thermal Diffusivity
λ	Wave Length
μ	Dynamic (Shear) Viscosity
ν	Kinematic Viscosity
ζ	Second (Bulk) Viscosity
$\tilde{\rho}$	Density
$\tilde{\Sigma}$	Viscous Stress Tensor
$\tilde{\omega}$	Angular Frequency of the Oscillation
$\tilde{\omega}_0$	Resonance Angular Frequency of the Mechanical Resonator
A_g	Cross-Sectional Area of the Gas Between the Stack
N_L	Laucret Number Related to Fluid
N_s	Laucret Number Related to Solid
A	Mach Number
Pr	Prandtl Number
W_0	Womersley Number

8. AKNOWLEDGEMENT

This work was supported by "Applied Physics Research Center of Sharif University of Technology". The authors wish to thank Hooshang Nayyeri for his assistance with the experiments.

9. REFERENCES

1. Sakamoto, Sh. I. and Watanabe, Y., "The Experimental Studies of Thermoacoustic Cooler", ***Ultrasonics***, Vol. 42, (2004), 53-56.
2. Garrett, S. L., "Resource Letter: TA-1: Thermoacoustic Engines and Refrigerators", ***Am. J. Phys***, Vol. 72, No. 1, (January 2004).
3. Petach, M., Tward, E and Backhaus, S., "Design of A High Efficiency Power Source (HEPS) Based on Thermoacoustic Technology", NASA/CR, (January 2004), 1-40.
4. Tijani, M. E. H.,"Loudspeaker-Driven Thermo-Acoustic Refrigeration", Ph.D. Thesis, Technische Universiteit Eindhoven, Eindhoven, Netherlands, (2001), 32-33.
5. Tao, J., Bao-Sen, Zh., Ke, T., Rui, B. and Guo-Bang, Ch., "Experimental Observation on A Small-Scale Thermoacoustic Prime Mover", ***Journal of Zhejiang University SCIENCE A***, Vol. 8, No. 2, (2007), 205-209.
6. Hofler, T. J., Adeff, J. A., "A Miniature Thermoacoustic Refrigerator", ***For ICs. Proceedings of 17th International Congress on Acoustics***, Roma, Italia, (2001), 45-47.
7. Jin, T., Fan, L., Wang, B. R. and Chen, G. B., "PZT Driven Miniature Thermoacoustic Refrigerator", ***Journal of Engineering Thermophysics***, (in Chinese), Vol. 25, No. 5, (2004), 776-778.
8. Liu, Y. C., "Study on the Miniaturization of Thermoacoustic Refrigerator", Ph.D. Thesis, Huazhong University of Science and Technology, Wuhan, China, (in Chinese), (2004), 10-15.
9. Symko, O. G., Abdel-Rahman, E., Kwon, Y. S., Emmi, M. and Behunin, R., "Design and Development of High-Frequency Thermoacoustic Engines for Thermal Management in Microelectronics", ***Microelectronics Journal***, Vol. 35, (2004), 185-191.
10. Rienstra, S. W. and Molenaar, J., "Systematic Derivation of Weakly Non-Linear Theory of Thermoacoustic Devices", Department of Mathematics and Computer Science, Technische Universiteit Eindhoven, Eindhoven, Netherlands, (February 2006), 1-16.
11. Landau, L. D. and Lifshitz, E. M. "Fluid Mechanics", 2nd Edition, Pergamon Press, Oxford, U.K., (1984), 210-297.
12. Seto, W. W., "Schaum's Outline Series Theory and Problems of Acoustics", McGraw-Hill Book Company, New York, U.S.A., (1970), 122-123.
13. Symon, K. R., "Mechanics", Addison Wesley, Massachusetts, U.S.A., (1971), 152-159.
14. Russel, D. A. and Weibull, P., "Tabletop Thermoacoustic Refrigerator for Demonstations", ***Am. J. Phys***, Vol. 70, No. 12, (December 2002), 1231-1233.
15. Piccolo, A. and Cannistraro, G., "Convective Heat Transport along a Thermoacoustic Couple in the Transient Regime", ***International Journal of Thermal Sciences***, Vol. 41, (2002), 1067-1075.